ELSEVIER

Biophysical Chemistry 134 (2008) 20–24

Biophysical Chemistry

http://www.elsevier.com/locate/biophyschem

Kinetic model for dynein oscillatory activity

B.N. Goldstein *, A.M. Aksirov, D.T. Zakrjevskaya

Institute of Theoretical and Experimental Biophysics Russian Academy of Sciences, 142290, Pushchino, Moscow Region, Russia

Received 20 November 2007; received in revised form 24 December 2007; accepted 26 December 2007
Available online 7 January 2008

Abstract

A kinetic model for dynein, a molecular motor, is considered. This model explains the oscillatory behaviour, observed by Chikako Shingyoji et al. [Ch. Shingyoji, H. Higuchi, M. Yoshimura, E. Katayama, T. Yanagida, Dynein arms are oscillatory force generators, Nature 393 (1998) 711–714.] and by Susumu Aoyama and Ritsu Kamiya [S. Aoyama, R. Kamiya, Cyclical interactions between two outer doublet microtubules in split flagellar axonemes, Biophys. J. 89 (2005) 3261–3268.] in surprisingly simple axonemal fragments. The model shows that sustained oscillations can be generated due to the obligate cooperative interaction of the two dynein heads in the axonemal fragments. No other feedback control interactions are involved in the model to explain oscillations, similar to those observed experimentally, for realistic dynein rate constants. The modified model shows how the ATP hydrolytic exhaustion influences the amplitude and frequency of dynein oscillatory activity.

Keywords: Dynein; Axoneme; Kinetic model; Oscillations; Cooperativity

1. Introduction

Dynein is a motor protein responsible for microtubule movements in cilia and flagella [3–6]. Despite many efforts, the fundamental unsolved problem till now is the mechanism of the oscillatory mechanical movement induced by dynein [2].

A number of models for this phenomenon have been proposed [7–13], based on the regulatory tension feedback in the axoneme (the core of flagella with many dynein molecules involved).

However, recent experimental observations [1,2] clearly demonstrate that a single dynein molecule can induce oscillatory movements in surprisingly simple axonemal substructures [14].

Therefore, it is necessary to consider a new model for the explanation of this phenomenon without invoking feedback regulation through the changeable axonemal curvature [1,2,14].

This paper considers such a model of oscillatory movements in simple axonemal fragments. Our model takes into account the known cooperative interactions of two dynein heads (two catalytic domains in a single dynein molecule), when they are binding to the microtubule [15].

A new model can be taken into account for explanation of axonemal beating and for waveforming movements in various motor systems, when being modified by including other regulatory interactions in the complex structures, involving many motor molecules.

This paper does not consider the complete theory of the axonemal movement, but considers only the reversible dissociation of simple axonemal fragments, which has been studied in the experiments [1,2]. Therefore, the problem of the direction of relative microtubule sliding is not concerned in our model.

We also consider various conditions for changeable or approximately constant ATP concentration, when ATP is the dynein substrate. The suspension of axonemal fragments has been perfused [2] with ATP in solution, or the photolysis of caged ATP has been used in the experiment [1]. We analyze how the ATP concentration decrease after a sudden increase influences the oscillation amplitude and frequency.

Fluctuations of the microtubule movement, in the presence of ATP, were negligibly small [1]. The observed oscillations can be considered as not stochastic but deterministic oscillations [1].

* Corresponding author. Fax: +7 8 4967 33 05 53.
E-mail address: goldstein@iteb.ru (B.N. Goldstein).

0301-4622/$ - see front matter © 2008 Elsevier B.V. All rights reserved.
doi:10.1016/j.bpc.2007.12.009

Therefore, the deterministic consideration of this phenomenon is used in our model.

2. Theory

Dynein is a protein of complex structure, forming the so-called "dynein arm" [6], which produces the microtubule movement by the motor domains ("dynein heads") [6]. Dynein motor domains use ATP as the energy source to produce the conformational changes and generate the mechanical microtubule movement.

Recent cryoelectronic tomography data [6] have revealed the molecular architecture and shapes of dynein arms.

Sea urchin dynein, the kinetics of which we model, has two motor domains in each dynein arm. Motor domains form parallel rings, which are positioned so they could act equivalently on the microtubule [6]. A motor domain (head) consists of different sub-domains and contains multiple nucleotide-binding sites [6]. One of these sites is the active site for ATP hydrolysis [7]. The role and the function of other sites is not exactly known [7]. Like other authors [13,15], we assume the two active sites of dynein to be equivalent.

Our kinetic model is a simplified version of the known model by Omoto et al. [15]. They have considered a four-state, two-site model to interpret the cooperativity of two dynein active sites. Their model for pseudo-steady-state conditions shows deviation of saturation kinetics from the Michaelis–Menten behaviour, which is the evidence of the active sites' cooperativity [15]. However, they did not take into account the time-dependent exhaustion of ATP in the local neighbourhood of dynein active sites, and did not include ATP diffusion. It could seem surprising that a simple modification of the dynein cooperative interaction model by introducing the substrate concentration as an additional variable in the differential equations without any other feedback regulations gives the explanation of the observed dynein activity oscillations.

Similarly to Omoto et al. [15], we apply mass-action equations for various dynein states participating in the mechano-chemical cycle. We do not use the probabilistic treatment, because only negligible stochastic noise was observed experimentally [1]. We consider the fractions of dynein molecules in the corresponding states as time-dependent variables in the deterministic kinetic equations.

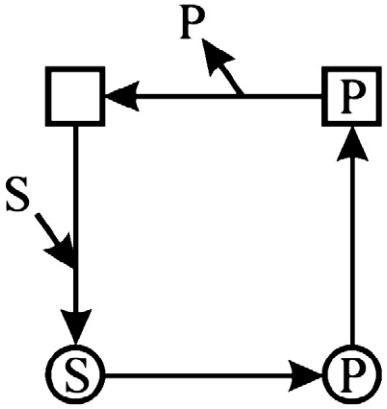

Fig. 1. Mechano-chemical four-state catalytic cycle for one head of dynein. Squares denote dynein associated with the microtubule, cycles denote dissociated dynein.

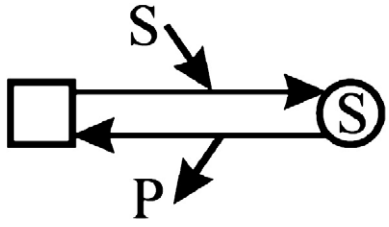

Fig. 2. Simplified two-state catalytic cycle for one head of dynein.

The following four states of the dynein catalytic cycle have been considered by Omoto et al. [15].

Fig. 1 shows only the forward direction of the catalytic cycle for one of two equivalent dynein heads. Here S is substrate (ATP), and P is product ($ADP+P_i$). In the presence of a sufficiently high ATP concentration the reverse reaction can be neglected [13].

Fig. 1 shows that each dynein head can be associated with the microtubule or dissociated (associated states are shown by squares, and dissociated by circles).

It is known that ATP bound at the active site of the dynein head induces its dissociation from the microtubule [15]. After ATP hydrolysis the dynein head reassociates, as shown in Fig. 1.

We consider the simplified catalytic cycle with only two most functionally important states of dynein: associated and dissociated, as shown in Fig. 2.

Fig. 2 shows the head dissociation from the microtubule combined with substrate (ATP) binding, as it is accepted in the literature [15]. The head association with the microtubule, substrate hydrolysis, and product release are also combined. The slowest of the last three steps is the product release [15].

For two dynein heads Fig. 2 is modified into Fig. 3.

Here, the substrate (ATP) binding at "left" and "right" heads is shown in the steps, $X_1 \rightarrow X'_2$ and $X_1 \rightarrow X''_2$. Product release is shown in the steps, $X'_2 \rightarrow X_1$ and $X''_2 \rightarrow X_1$. In state X_3 both active sites are occupied by the substrate.

The hydrolysis and product release steps are connected with mechanical movements [7]. Therefore, in accordance with the finding of [15], we suppose dynein active sites are cooperative in these steps. Namely, we suppose the dynein hydrolytic activity for both sites, occupied by ATP, differs from the activity of a single site when the second site is free.

Our model includes also the reversible dynein–microtubule association, which can proceed without ATP participation in the active sites. This slow process should be taken into account

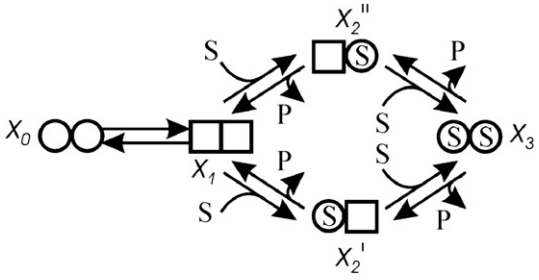

Fig. 3. Kinetic scheme for dynein with two heads.

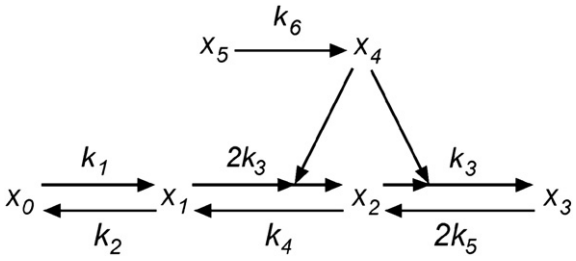

Fig. 4. Kinetic graph for dynein with two equivalent heads and the substrate influx, $X_5 \rightarrow X_4$.

[15], and its forward and reverse rates can depend on transverse forces (t-forces) [10,11]. The t-force acts to pry microtubules apart or pushes them together in different conditions [10,11].

Moreover, non-productive ATP or ADP binding at the non-active nucleotide-binding dynein sites can induce such slow reversible dynein–microtubule association [7].

The two mechanisms of slow dynein–microtubule interaction (with or without non-productive nucleotide binding) are equivalent in their effect on the oscillatory kinetics [16]. Therefore, we consider in the model only one of these mechanisms. This is represented in Fig. 3 by the reversible transition, $X_0 \Leftrightarrow X_1$.

The minimal kinetic scheme for dynein presented in Fig. 3, obviously, can be more detailed. However, any more detailed scheme can only complicate the kinetic behaviour. Our aim is to explain the observed dynein oscillatory behaviour using a model that is as simple as possible without involving any additional feedback control.

3. Results

3.1. Model 1 (Constant substrate influx)

We use the graph-theoretical approach [17] to analyze the ability of kinetic schemes, obeying the mass-action law, to generate oscillations. Only schemes of certain topological structure (involving branched cycles, constructed from the reaction steps) can generate oscillations (see [16] for an example). All reaction participants, including enzyme and substrate in various states, are represented as nodes of a graph.

The scheme of Fig. 3 is represented by the kinetic graph in Fig. 4.

This graph is similar to the graph analyzed in our preliminary work [16], where the values of the kinetic parameters in the oscillatory domain have been estimated.

Here we combine the identical steps for substrate (X_4 in Fig. 4) binding at "left" and "right" dynein head by introducing the combined dynein state, $X_2 = X'_2 + X''_2$, with one of two equivalent sites occupied by substrate, X_4.

The step combination leads to the twice greater rate constants, as shown in Fig. 4.

Model 1 involves the approximately steady substrate influx (diffusion), shown in Fig. 4 as $X_5 \rightarrow X_4$, where X_4 is the substrate (ATP) in the neighbourhood of dynein active sites, and X_5 is the substrate (ATP) in the source at an approximately constant concentration. This is a simplification of the real system, where the substrate concentration in the bulk suspension slowly changed during the diffusion to the dynein active sites [1].

Here various k_i are the rate constants, X_0, X_1, X_2, X_3 are the dynein states, X_4 and X_5 represent the two substrate' states.

The following kinetic equations correspond to the graph in Fig. 4.

$$\begin{aligned}
\frac{dx_1}{dt} &= k_1 x_0 - k_2 x_1 - 2k_3 x_1 x_4 + k_4 x_2 \\
\frac{dx_2}{dt} &= 2k_3 x_1 x_4 - k_4 x_2 - k_3 x_2 x_4 + 2k_5 x_3 \\
\frac{dx_3}{dt} &= k_3 x_2 x_4 - 2k_5 x_3 \\
\frac{dx_4}{dt} &= v_6 - 2k_3 x_1 x_4 - k_3 x_2 x_4
\end{aligned} \qquad (1)$$

Eq. (1) are written according to mass-action law, where x_i is the molecular fraction of the participant, X_i.

The normalized fractions of the dynein states, $x_i = [X_i]/[E]$, are interconnected in Eq. (2):

$$x_0 + x_1 + x_2 + x_3 = 1. \qquad (2)$$

We solved Eqs. (1) and (2) using the program DBSolve [18] to obtain the oscillatory solution at certain parameter values. For this calculation we used values of the rate constants close to those known from the literature.

The constants, k_1 and k_2, characterize the reversible dynein–microtubule association without nucleotide participation. The rate of this slow process depends on various conditions. There can be $k_1 > k_2$ or $k_1 < k_2$ [2].

Our preliminary analysis [16] shows that the sustained oscillations can be obtained at $k_1 < k_2$ only. Therefore, we assume that the realistic values for these parameters can be accepted as $k_1 = 1\ s^{-1}$, $k_2 = 10\ s^{-1}$.

The substrate (ATP) binding at a single dynein active site, according to [15], can proceed with the rate constant $k_3 = 5 \times 10^4\ M^{-1}\ s^{-1}$.

The approximately constant substrate influx in Model 1 is estimated in accordance with data [1] as having the rate, $v_6 = k_6 [X_5] = 100\ \mu M\ s^{-1}$. Here $[X_5]$ denotes the approximately constant ATP concentration in the source, and k_6 is the rate constant for ATP diffusion through the suspension of axoneme fragments.

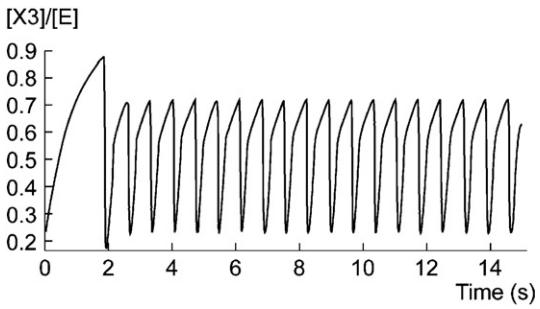

Fig. 5. Oscillatory dynein dissociated fraction, $x_3 = [X_3]/[E]$, calculated according to Eqs. (1) and (2), Model 1, for parameters, shown in text ($k_5 = 75\ s^{-1}$). Initial values: $x_1(0) = x_2(0) = x_4(0) = 0$, $x_3(0) = 0.25$.

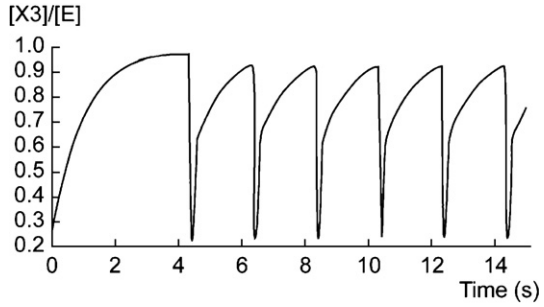

Fig. 6. Oscillations as in Fig. 5 for changed $k_5=60\ s^{-1}$.

The rate constants, k_4 and k_5, characterize the mechanical work combined with the ATP hydrolysis [15]. Their estimation is made in accordance with data of [15]. We accept $k_4=300\ s^{-1}$ and $k_5<k_4$ to describe the cooperative interaction of the dynein heads, which has been investigated by Omoto et al. [15]. We use different values for k_5 to demonstrate how different cooperativity influences on the dynein kinetic behaviour.

Fig. 5 shows oscillations of the calculated dynein fraction, $x_3=[X_3]/[E]$, in the dynein state, X_3, in which both dynein heads are dissociated from the microtubule. The parameter value $k_5=75\ s^{-1}$ is used in Fig. 5.

Fig. 6 demonstrates oscillations, as in Fig. 5, but with $k_5=60\ s^{-1}$.

One can see from Figs. 5 and 6 that the oscillation frequency is changed with the changed cooperativity of interacting dynein heads.

Fig. 7 shows how the oscillation period for Model 1 depends on the parameter relation, k_5/k_4, $k_4=300\ s^{-1}$. One can see that sustained oscillations exist in the parameter domain, $0.16<k_5/k_4<0.27$, and the oscillation period is less for greater k_5 values.

The relation, $k_5/k_4<1$, could be interpreted as the negative cooperativity (anticooperativity). However, at pseudo-steady-state conditions considered in [15], the saturation kinetics is characterized by the apparent substrate binding constants, k_3/k_4 and k_3/k_5. In this case the condition, $k_3/k_4<k_3/k_5$, is interpreted as "apparent positive cooperativity" [15]. It is interesting that the dynein cooperativity [15] is needed to observe oscillations.

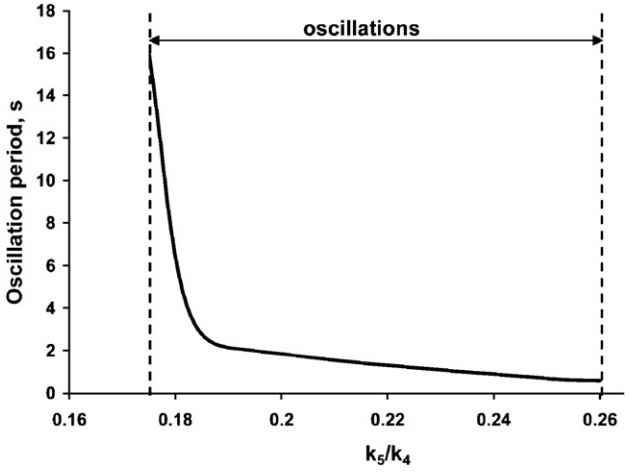

Fig. 7. Dependence of the oscillation period on the cooperativity parameter, k_5/k_4, calculated forModel 1, $k_4=300\ s^{-1}$, other parameters as in Figs. 5 and 6.

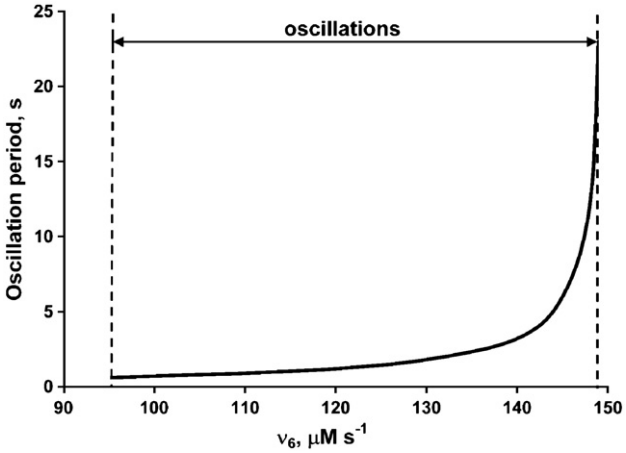

Fig. 8. Dependence of the oscillation period on the constant substrate influx value, v_6, calculated forModel 1. Other parameters as in Figs. 5 and 6.

One can conclude that the obligatory dynein cooperativity is the condition for dynein activity oscillations.

Fig. 8 shows how the oscillation period for Model 1 changes when v_6 is changed. The sustained oscillations are obtained in the domain, $90<v_6<150$, μM s^{-1}. One can see that the oscillation period is less for lower v_6 values.

In the experiments [1] the oscillation period was growing during the initial time. Therefore, we introduce into the model the initial increase in the bulk substrate concentration due to the diffusion from the source. This model modification leads us to Model 2, which describes the experimental data [1].

3.2. Model 2 (Substrate exhaustion)

The initial ATP concentration in the source was decreasing in the experiment [1] from its value about 1000 μM due to the hydrolysis by dynein. This decrease was observed in parallel with the increase in the oscillation period [1].

To describe this phenomenon, which differs from that of Fig. 8, we introduce an additional ATP state into the graph of Fig. 4:

$$X_6 \xrightarrow{k_7} X_5 \xrightarrow{k_6} X_4 \qquad (3)$$

Here, X_6, X_5, and X_4, represent the substrate, (ATP), in the source, in the bulk suspension, in the neighbourhood of the active sites, at

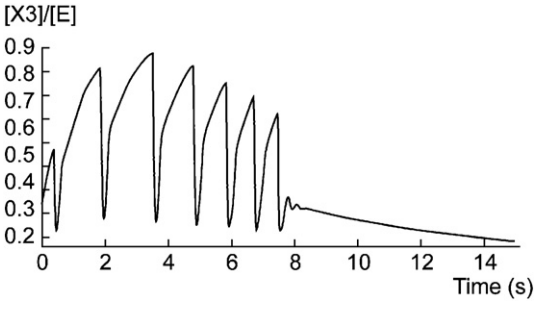

Fig. 9. Similar dependence as in Fig. 5, calculated according to Eqs. (1), (2), and (4), Model 2, for parameters, shown in text $k_5=50\ s^{-1}$. Additional parameters: $k_6=0.7\ s^{-1}$, $k_7=0.1\ s^{-1}$, $x_5(0)=45$ μM, $x_6(0)=1000$ μM.

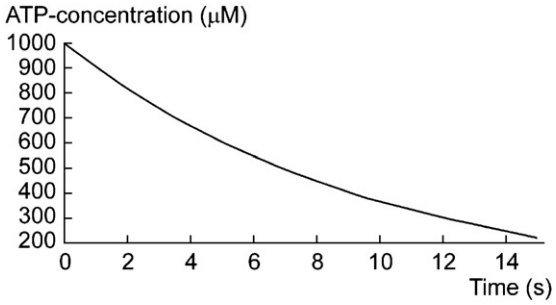

Fig. 10. Decreasing ATP concentration, $x_6=[X_6]=[\mathrm{ATP}]$, calculated for Model 2 with parameters shown in Fig. 9.

concentrations, correspondingly, x_6, x_5, and x_4. These substrate states are present at different time-dependent concentrations with initial values, $x_6=1000$ μM, $x_5=45$ μM, $x_4=0$.

The initial increase in x_5 induces the increased influx to the dynein active sites thereby increasing the oscillation period.

Parameters, k_7 and k_6, represent in Model 2 the diffusion rates. We accept their values to be rather small:

$$k_6 = 0.7\,\mathrm{s}^{-1}, k_7 = 0.1\,\mathrm{s}^{-1}.$$

Taking in mind the additional process (3), we add the following equations to Eq. (1):

$$\begin{aligned} \frac{dx_5}{dt} &= -k_6 x_5 + k_7 x_6 \\ \frac{dx_6}{dt} &= -k_7 x_6 \end{aligned} \quad . \tag{4}$$

The system of Eqs. (1), (2), and (4) was solved with using the program DBSolve [18] for parameter values and initial concentrations shown in the legend to Fig. 9.

Fig. 9 shows the calculated oscillations for Model 2, qualitatively similar to the experimentally observed oscillations of the dynein activity [1]. It is seen that the oscillation period initially becomes greater, then smaller. Only the initial part, including more periods, was observed experimentally [1].

Fig. 10 shows the calculated substrate concentration, $[\mathrm{ATP}]=[X_6]$, which falls with time similarly to that observed in the experiment [1]. Therefore, Model 2 describes more adequately the observed phenomenon than Model 1.

4. Discussion

The known models for flagellar beating do not consider a single dynein molecule as the generator of oscillations, because such a simple system seems not to have the necessary regulatory feedback.

However, the recent experiments have demonstrated the oscillatory movement in surprisingly simple axoneme fragments [1,2].

Therefore, we consider here the dynein molecules, reversibly complexed with microtubule fragments, as the generators of the observed oscillations.

It may not seem obvious that the apparent positive cooperativity in the functioning of the dynein heads, observed by Omoto et al. in pseudo-steady-state saturation kinetics [15], can produce the feedback regulation necessary for oscillations. However, the known cooperativity of dynein heads is shown here to produce kinetic parameter values necessary for dynein activity oscillations.

We also consider in our models various simplified conditions for substrate (ATP) exhaustion, observed in the experiment [1]. The calculated curves demonstrate the dynein oscillatory movement similar to observed experimentally [1].

The aim of this paper is to show that the substrate hydrolytic exhaustion can change the oscillation frequency in a way observed by the authors of the experimental work [1].

Moreover, we demonstrate by our models that the oscillation frequency depends strongly on the strength of the dynein heads interaction. This interaction can be regulated in the full axoneme by various additional interactions, which we do not analyze here.

References

[1] Ch. Shingyoji, H. Higuchi, M. Yoshimura, E. Katayama, T. Yanagida, Dynein arms are oscillatory force generators, Nature 393 (1998) 711–714.
[2] S. Aoyama, R. Kamiya, Cyclical interactions between two outer doublet microtubules in split flagellar axonemes, Biophys. J. 89 (2005) 3261–3268.
[3] S.A. Burgess, P.J. Knight, Is the dynein motor a winch? Curr. Opin. Struct. Biol. 14 (2004) 138–146.
[4] M.P. Koonce, M. Samso, Of rings and levers: the dynein motor comes of age, Trends Cell Biol. 14 (2004) 612–619.
[5] K. Oiwa, H. Sakakibara, Recent progress in dynein structure and mechanism, Curr. Opin. Cell Biol. 17 (2005) 98–103.
[6] D. Nicastro, C. Schwartz, J. Pierson, R. Gaudette, M.E. Porter, J.R. McIntosh, The molecular architecture of axonemes revealed by cryoelectron tomography, Science 313 (2006) 848–944.
[7] Y.Q. Gao, A simple theoretical model explains dynein's response to load, Biophys. J. 90 (2006) 811–821.
[8] C.J. Brokaw, Computer simulation of flagellar movement: conventional but functionally different cross-bridge models for inner and outer arm dyneins can explain the effects of outer arm dynein removal, Cell Motil. Cytoskel. 42 (1999) 134–148.
[9] N.J. Cordova, B. Ermentrout, G.F. Oster, Dynamics of single-motor molecules: the thermal ratchet model, Proc. Natl. Acad. Sci. U.S.A. 89 (1992) 339–343.
[10] Ch.B. Lindemann, L.J. Macauley, K.A. Lesich, The counterbend phenomenon in dynein-disabled rat sperm flagella and what it reveals about the interdoublet elasticity, Biophys. J. 89 (2005) 1165–1174.
[11] Ch.B. Lindemann, Structural–functional relationships of dynein, spokes, and central-pair projections predicted from an analysis of the forces acting within a flagellum, Biophys. J. 84 (2003) 4115–4126.
[12] R.A. Cross, The kinetic mechanism of kinesin, Trends Biochem. Sci. 29 (2004) 301–309.
[13] N. Thomas, R.A. Thornhill, The physics of biological molecular motors, J. Phys. D: Appl. Phys. 31 (1998) 253–266.
[14] A.J. Hunt, Keeping the beat, Nature 393 (1998) 624–625.
[15] Ch.K. Omoto, J.S. Palmer, M.E. Moody, Cooperativity in axonemal motion: analysis of a four-state two-site kinetic model, Proc. Natl. Acad. Sci. U.S.A. 88 (1991) 5562–5566.
[16] B. Goldstein, Switching mechanism for branched biochemical fluxes: graph-theoretical analysis, Biophys. Chem. 125 (2007) 314–319.
[17] B.N. Goldstein, A.I. Ivanova, Hormonal regulation of 6-phosphofructo-2-kinase/fructose-2,6-bisphosphatase: kinetic model, FEBS Lett. 217 (1987) 212–215.
[18] I.I. Goryanin, T.C. Hodgman, E.E. Sel'kov, Mathematical simulation and analysis of cellular metabolism and regulation, Bioinformatics 15 (1999) 749–758.